Improved FDCM in Laser Scanning Inspection System for Workpiece Deformation

Yibin Huang, Yue Guo

Institute of Automation, Chinese Academy of Sciences

University of Chinese Academy of Sciences

Beijing, China

{huangyibin2014, guoyue2013}@ia.ac.cn

Kui Yuan

Institute of Automation, Chinese Academy of Sciences

University of Chinese Academy of Sciences

Beijing, China

Abstract —**Three-dimensional (3D) inspection based on machine vision is high-precision and efficient. In this paper, a laser scanning system using the triangulation measurement is designed to obtain dense point clouds of the workpiece surface, and the point clouds are projected to two-dimensional (2D) range images. Fast Directional Chamfer Matching (FDCM) is a reliable algorithm for object detection and localization, and it is improved to accelerate the time-consuming 3D registration. Although the author of FDCM greatly improved the directional chamfer matching, it remains very slow in practice. We mainly improved the line fitting process and distance transform in this algorithm, and they greatly accelerate the scanning process. Experimental results show that the scanning system with the improved algorithm can highlight the deformation of the workpiece in real time.**

Index Terms—*Fast Directional Chamfer Matching; inspection; laser Scanning; registration.*

I. INTRODUCTION

Driven by the market, 3D machine vision quality control is becoming increasingly important [1]. 3D imaging device design and point cloud registration are the main research contents for scholars.

3D imaging methods include laser line scanning, structured light, multi-view vision, time of light and so on. It is worth noting that the principle of laser line scanning is relatively simple, and this point cloud obtaining method has many advantages such as high-speed and high-precision, and it is not affected by light conditions. Therefore, it is widely used in the quality inspection in production lines, and the structure, the principle, and the calibration method of the laser scanning inspection system are mainly introduced in Section II.

Many researchers has focused on how to align one point cloud to another. Specifically, the most popular registration algorithm is the ICP (Iterative Closest Point) [2]. In general, with a proper initial transformation matrix, good registration can be obtained using ICP. However, the solution of ICP may be easily trapped in local optimum, and this algorithm is time-consuming. A large number of ICP variants were proposed by optimizing the iteration to shorten the registration time or finding an initial transformation matrix [3, 4]. Another widely used registration algorithm is the NDT (Normal Distribution Transform) [5]. In NDT, a simple description of the probability density distribution function model turns the registration problem to a typical optimization problem. NDT is faster than ICP, since it does not have to find corresponding points, but an initial transformation matrix is also required and sometimes the solution may be trapped in local optimum in NDT. Applying features in local or those in global for registration is also a trend [6, 7], but it is hard to adapt these algorithms to point clouds in different density, size, and noise or lack of features.

Registration from a 2D range image is also common for a 3D point cloud, and it improves the most time-consuming content in FDCM [8] which becomes a real-time 2D localization algorithm, then it is applied to the registration of the point cloud in section IV, which simplifies the complex registration, and the experimental result demonstrates the practicability of our method in laser scanning point cloud registration.

II. LASER SCANNING INSPECTION SYSTEM

The laser scanning inspection system consists of a linear laser projector, a charge-coupled device (CCD) camera and a moving platform. As shown in Fig.1, a world coordinate system is on the face of the moving platform which X_W-O_W-Y_W plane is right on the surface, and Y_W axis is parallel to the scanning direction. The laser-line projector is mounted upon the moving platform, and we do our best to make sure the light plane is almost parallel to the X_W-O_W-Z_W axis.
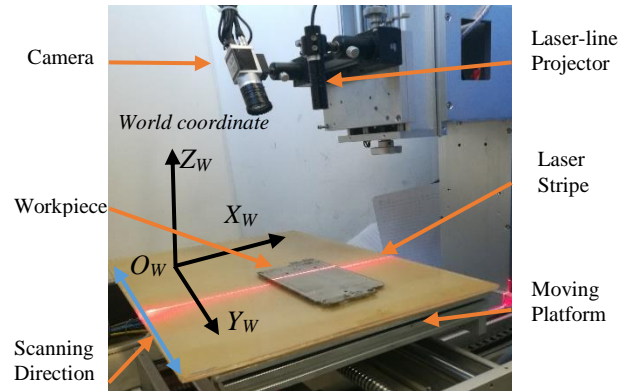

Fig. 1 Overview of the system.

A. Triangulation ranging

Most of machine vision measurements are based on the triangulation theory. Specifically, the laser line (laser stripe) is projected to the image frame, as shown in Fig.2. Three coordinate systems are established: the world coordinate system we have discussed before, the image coordinate system u-o-v, and the camera coordinate system, which the origin O_C is right on the focal point of the camera.
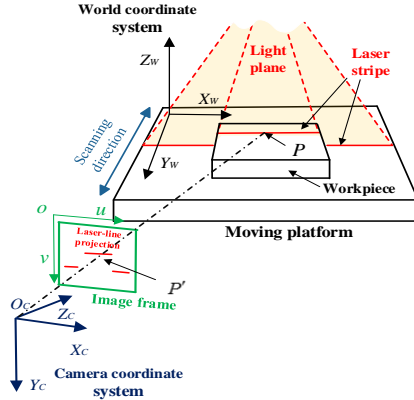

Fig.2 Triangulation ranging.

At this time, the point P on the stripe, which coordinate is (X_W, Y_W, Z_W), is projected to the point $P'(u, v)$, thus the 3D coordinate can be estimated given the function:

$$(X_W, Y_W, Z_W) = f(u, v) \qquad (1)$$

The point P in the camera coordinate system is (X_C, Y_C, Z_C), according to the principle of pinhole imaging, we have the equation as follows:

$$Z_C \begin{bmatrix} u \\ v \\ 1 \end{bmatrix} = \begin{bmatrix} fu & 0 & u_0 \\ 0 & fv & v_0 \\ 0 & 0 & 1 \end{bmatrix} \begin{bmatrix} X_C \\ Y_C \\ Z_C \\ 1 \end{bmatrix} \qquad (2)$$

In this paper, to simplify our model, we assume that all the distortions in the image have been corrected. In (2), fu and fv are the focal lengths, and (u_0, v_0) is the optical central position, thus all the parameters are intrinsic parameters of the camera. (2) can be overwritten as:

$$X_C = Z_C(u - u_0) / fu \qquad (3)$$

$$Y_C = Z_C(v - v_0) / fv \qquad (4)$$

and the light plane can be decribed with:

$$Z_C = a_1 + a_2 X_C + a_3 Y_C \qquad (5)$$

where a_1, a_2 and a_3 are constants used to determine the light plane. Combine (3), (4), and (5), we get:

$$Z_C = \frac{a_1}{[1 - a_2(u - u_0) / fu - a_3(v - v_0) / fv]} \qquad (6)$$

The transformation equation from the world coordinate system to the camera system can be defined as:

$$\begin{bmatrix} X_C \\ Y_C \\ Z_C \\ 1 \end{bmatrix} = \begin{bmatrix} R & t \\ 0^T & 1 \end{bmatrix} \begin{bmatrix} X_W \\ Y_W \\ Z_W \\ 1 \end{bmatrix} = M \begin{bmatrix} X_W \\ Y_W \\ Z_W \\ 1 \end{bmatrix} \qquad (7)$$

where the matrix $[R|t]$ or M called extrinsic parameter matrix. (6) can be overwritten as

$$\begin{bmatrix} X_W \\ Y_W \\ Z_W \\ 1 \end{bmatrix} = M^{-1} \begin{bmatrix} X_C \\ Y_C \\ Z_C \\ 1 \end{bmatrix} \qquad (8)$$

B. Light plane calibration

Camera calibration is an important step in computer vision, and the most commonly used method is Zhang's method, and Zhang also provides an open source camera calibration toolbox [9]. Specifically, about 20 good quality pictures of a planar checkerboard are taken, and the intrinsic parameters of the camera can be easily obtained with the toolbox, so we skip the details of this step.
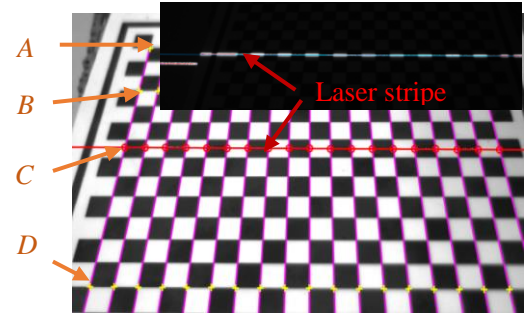

Fig.3 The intersection points of the checkerboard and the laser stripes.

In Fig.3, we put a checkerboard under the camera and take two pictures (one with the laser projector on and the other with the projector off). Then we extract all the corner coordinates on the checkerboard and the laser stripe center line. Based on the projective geometry, corners including A, B, and D and an intersection C fix the constraint:

$$r = \frac{AC}{CB} / \frac{AD}{DB} \qquad (9)$$

where r is the cross-ratio, and this constraint is called the invariance of cross-ratio. It means that r is always a constant, regardless of the line segment lengths of AC, CB, AD, and DB are measured on the world coordinate system or the image coordinate system. The image coordinate (u, v) of point C can be calculated through the intersection of the pink line and the red line (the laser stripe), then the world coordinate (X_W, Y_W, Z_W) of point C can be calculated with the (8). The extrinsic matrix M can be provided with the camera calibration toolbox. So the camera coordinate (X_C, Y_C, Z_C) of point C can be calculated with (7). There exists 19 intersections in an image, then we save these 3D coordinates and change the position of the calibration plate, repeat the steps described above several times, so we get dozens of 3D points. Fitting these points into a plane with the least square method, then we get a light plane, and parameters

of the plane a_1, a_2, and a_3 in (5) are estimated. Finally, the function f in (1) can be defined with (1) - (8).

The stripe center is extracted with the gray centroid method. When we are sampling data, 3D coordinates of the laser stripe center are recorded. X_W and Z_W are calculated using the above method, but Y_W is replaced by the current displacement of the platform.

C. System performance

To test the system accuracy, a set of Grade 0 (error within $1\mu m$) gage blocks are used, as shown in Fig.4. The measurements are repeated 20 times, and the mean height is calculated as the metric. The actual heights of block 1, block 2, and block 3 are h_1=1.005 mm, h_2=3.000 mm, and h_3=10.000 mm, while the corresponding measurements are h_1'=1.0025 mm, h_2'=3.0036 mm, and h_3'=10.0037 mm. To this end, the maximum measurement error is:

$$err_{max} = |(h_3 - h_1) - (h_3' - h_1')| = 0.0362mm,$$

and the maximum measurement variance is 0.0011 mm. Therefore, the accuracy of the laser scanning inspection system is about 0.04 mm.
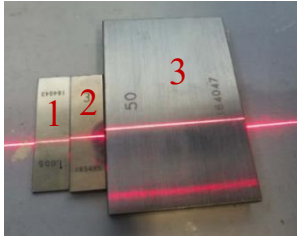

Fig.4 Measurement accuracy test.

The camera in use is *Basler Aca-1600-20gm*, which has a CCD sensor of 1600*1200 pixels. This camera supports reading ROIs (Region of Interest), and the frame rate can be increased, specifically, the frame rate of the camera can reach 70 *fps* (frames per second) although its designed frame rate is 20 *fps*. A 1600*196 light stripe image can be transformed to 3D data within 2 *ms* with an Intel i5-4core-3.3GHz CPU. In other words, the image processing speed can reach 500 *fps* if the frame rate is set fast enough.

III. IMPROVED FAST DIRECTIONAL CHAMFER MATCHING

A. Fast directional chamfer matching

Workpieces on production lines always lack texture features, but their edge features are relatively stable. Based on this characteristic, Mingyu-Liu recommended us to use Fast Directional Chamfer Matching (FDCM) to estimate the poses of the workpieces [8]. FDCM is an algorithm improved from Directional Chamfer Matching (DCM). DCM matches the template and the query image based on the distance and the direction of edges. Let $U=\{u_i\}$ and $V=\{v_j\}$ be the template sets and the query image edge maps respectively, the chamfer distance between U and V is given by the average of distances between each point $u_i \in U$ and its nearest edge in V:

$$d_{DCM}(U,V) = \frac{1}{n}\min_{v_j \in V}(|u_i - v_j| + \lambda|\phi(u_i) - \phi(v_i)|) \quad (11)$$

where $n=|U|$, and λ is a weighting factor, and $\phi(x)$ means the edge direction at x. To accelerate the algorithm, the general practice contains evenly quantizing the edge orientation into k directions and implementing distance transform to simplify the calculation. The matching process includes sliding the template to scan the entire query image and calculating the chamfer distance (d_{DCM}) at each position, when the lowest score or the score below a certain threshold exists at such a position, it suggests that there is a target. The complexity of the DCM is:

$$O(kn) + O(|V|) \quad (12)$$

Based on DCM, Liu made the following improvements:

1) Line segments expression: A RANSAC line fitting algorithm is used to approximate the template and the query edge image to line segments. If a set of points have cardinality n, and their linear representation have only m line segments, so only m memories are required to store points ($m << n$), and such an expression is much more concise.
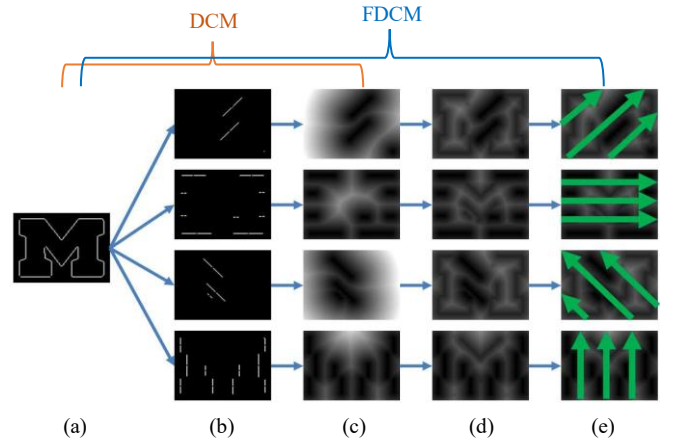

Fig.5 The distance transform tensor computation of DCM and FDCM.

(a) The set V in the query edge map (DCM) and line segments (FDCM). (b) Edges are quantized into discrete orientation channels. (c) Distance transform of each orientation. (d) Distance transform is updated based on the orientation cost. (e) The Distance transform is integrated along the discrete edge orientations.

2) Integral distance transform: In Fig.5, every edge in (a) is split into k orientations in (b) and the corresponding 2D distance transform in (c) is computed. The orientation is regarded as the third dimension, and its cost is updated to the distance transform tensor in (d). At last, the integral distance transform along each orientation is computed in (e). When sliding line segments of the template on the query image, the cost d_{DCM} can be computed as:

$$d_{DCM}(U,V) = \frac{1}{n}\sum_{l_j \in L_U}|IDT3_V(e_j,\phi_j) - IDT3_V(s_j,\phi_j)| \quad (12)$$

where the $L_U=\{l_j\}_{j=1...m}$ is the linear representation of template edge points U, $IDT3_V(x, \phi)$ is the integral distance transform tensor at orientation ϕ; s_j, e_j, and ϕ_j are the starting location, the ending location, and the orientation of the jth line segment l_j respectively. (12) demonstrates that the integral distance transform accelerates the cost computation because it has only a few arithmetic operations.

3) Region search optimization: If the chamfer distance cost of a location is much larger than the cost of the target location, it is impossible to have a target within a certain nearby region. Skipping these regions can greatly accelerate the search process. A full search requires linear time, but the optimized region search only requires sub-linear time.

Although FDCM can find the target in the sub-linear time, this method cannot work in real time. There are two time-consuming steps including the line fitting and the distance transform tensor computation. Improvement of the algorithm is imperative.

B. Replace the line fitting method

The line fitting method in FDCM is a variance of the RANSAC algorithm, and the fitting steps can be described as follows:

1) Compute an edge image (for example, canny edges).

2) Pick several points in the edge image randomly, and each point and its orientation define a line.

3) The support of each line includes points in the edge that are closed to the line, and these points are connected.

4) The line segment with the greatest support is retained if it has enough points.

5) Repeat *1) - 4)* on the remaining points until there are not enough points to support any new lines.

The line randomly generated in step *1)* that has too low probability to find a strong support leads to many false attempts, and the following steps will be very time-consuming.

Line Segments Detector (LSD) [10] is a fast and robust line extraction algorithm. The main idea of LSD can be shown in Fig.6. The main task of LSD is to find line segments in a grayscale image where the gradient is strong. The key is to find the rectangular support regions where the elements share the same gradient direction or line support regions. If the line support region has enough elements, a line segment is detected. It is a very feasible method that starts searching the line support regions from gradient maximum. Therefore, it is necessary to sort the gradient values after the gradient image is computed. A pseudo sorting method is used by throwing gradient values into a series of uniformly distributed bins, and it reduces the sorting complexity from $O(n\log(n))$ to linear time.
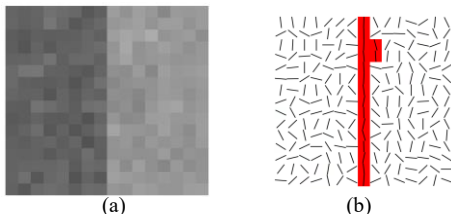

Fig.6 Line support regions search

(a) Grayscale image. (b) Gradient image, short line segments are the gradients of the corresponding pixels, the red rectangular region is a line support region suggest that there is a line segment.

C. Angular Voronoi diagram

The continuous angle is quantified into k discrete orientations. In each orientation, a distance transform image, a 3D distance transform image, and an integral distance transform image are calculated. So $3*k$ times pixel traversal of the query image is required. The author of FDCM suggests that 60 orientations are sufficient. However, 180 times pixel traversal is very time-consuming. In addition, the angle discretization will lose some angle accuracy.

Instead of dividing the angle into k discrete orientation, we calculate an angular Voronoi diagram. The angle of a pixel is assigned by the inclination angle of its closest line segment. In Fig.7 (c), the Voronoi diagram is computed, different color regions represent different angles. In the matching process, the distance between the template and point sets in the query image can be obtained from the 2D distance transform tensor, the angular cost can be computed by the template line and the Voronoi diagram, the chamfer distance can be computed by:

$$d_{DCM}(U,V) = \frac{1}{n} \sum_{l_j \in L_U} \sum_{p_i \in l_j} [DT(p_i) + \lambda \mid \phi_j - VD(p_i) \mid] \quad (13)$$

where p_i means the ith point belonging to the line l_j, ϕ_j is the orientation of l_j, DT and VD are the distance transform image and Voronoi image respectively. Only two tensors are necessary, making our method $k*3/2$ times faster than FDCM.
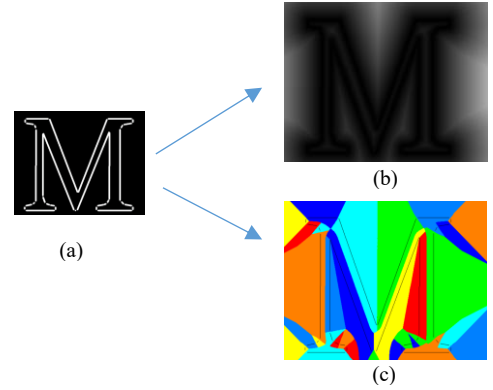

Fig.7 Distance transform and angular Voronoi diagram

D. Line based matching

The matching process of DCM is a brute force search. For a $r*c$ query image with k directions, there are $r*c*k$ candidate locations, and the number of locations often reaches millions, although such a number is reduced in FDCM by skipping some nearby regions, it is still large. Since the line segment is a stable feature, lines that have similar length to the template are searched.

Firstly, sort the lines of the template and those of the query image from long to short respectively. Template lines are rotated and translated such that the longest template line segment is aligned with one line segment in the query image which has similar length, as shown in Fig.8. The template is translated to that position and the cost is evaluated to decide whether there is a target. If no targets are found with the longest line segment of the template, then a new search begins using the second longest counterpart. If there is a target, it is usually found before the fifth longest line segment is used. The number of candidate locations drops from millions to thousands (even dozens).

The running time depends on how complex the background is and what size the image is. We compare the consumed time using our method and that using the code of FDCM provide by the author [11]. Our method runs 24 times faster than FDCM does in this case, as listed in TABLE I. If the background is cleaner, the processing speed of our method can reach 30 *fps*.

Template image

Query image   Target is found
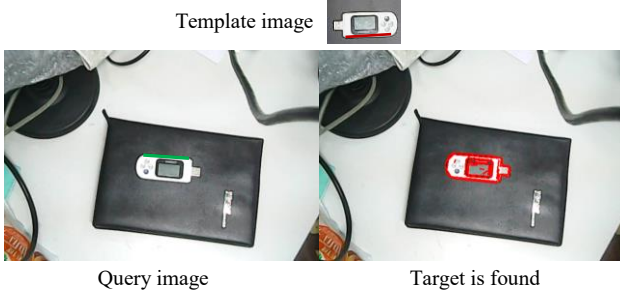
Fig.8 Line based matching.

Find the line segments which similar to the template (left). The cost is lower than the threshold and the target is found (right).

TABLE I
COMPARISONS OF THE RUNNING TIME

Algorithm	Line fitting	Distance transform	Matching
FDCM	978.834	889.371	62.448
This paper	28.755	5.456ms	48.464

Our algorithm requires no training processes, it only needs a template image. In general, only a global chamfer distance threshold is needed to be changed after replacing the template. As shown in Fig.9, the target can be detected and localized under the partial occlusion (a), in the cluttered background (b), and in bad illumination (c). It is also suitable for the objects with only a few line segments, for example, the mouse in (d). Therefore, the improved FDCM is robust and usable.

Fig.9 The matching performances of our method.

IV. REGISTRATION

The object defect to be inspected in this paper is the deformation of the workpiece. The workpiece is a very thin metal sheet for a cellphone, and it is easy to be deformed during die casting. Only by comparing with the standard piece or its CAD model, can we know whether the workpiece is qualified. The point cloud registration can be described as:

$$C_{target} = [R_3 \mid t_3]C_{source} \qquad (14)$$

where C_{source} and C_{target} are the source point cloud and the target point cloud respectively; R_3 and t_3 are the rotation matrix and translation matrix from the source point cloud to the target point cloud. The target of the registration is to estimate this two matrix.

ICP and NDT handle registrations in the 3D space, which are proved to be relatively slow. Applying 2D shapes to 3D registration is also a practical approach. 2D shapes or features that have lower dimensions and less data lead to a much faster registration. 3D point clouds can also be transformed to the 2D range image, and [12] demonstrates how to transform point clouds generated from a laser scanner to a range image. The Range image is also known as the depth image, the pixel value in the range image means the distance from the scene to a reference frame, and the reference frame in this paper is the plane in the world coordinate system (Z_W=0). The range image is shown as a pseudo color image in Fig.10.

In [13], 2D points on the contours in the range image is used to perform ICP registration, since contour points are far less than the whole point cloud, our registration is much faster. Shape Base Matching (SBM) is widely used in 2D matching or registration [14], the shape (contour) of the template is used for the image matching. Qin proposed a Contour Primitives of Interest Extraction (SPIE) method [15], which extracts some line segments and some circular arcs to conduct the 2D pose estimation.
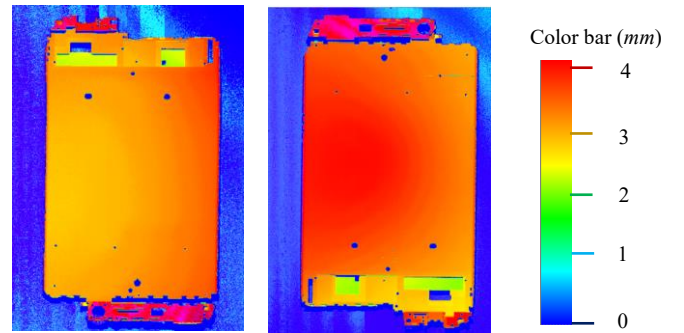

Color bar (*mm*)

Fig.10 The reference workpiece and one to be inspected

There exist two workpieces in Fig.10: the left piece is a qualified one used as the reference (target image) and the right is a workpiece to be inspected (source image). Now we compare these methods to our method discussed in the previous section. The differences of these methods are shown in TABLE II

TABLE II
COMPARISON OF REGISTRATION ALGORITHMS.

Method	Features used	Time (ms)	drawback.
ICP	1011188 3D points, initial transform matrix	8650.993	Time-consuming
NDT	1011188 3D points, initial transform matrix	3554.329	Time-consuming
2D ICP	6892 2D points, initial transform matrix	39.374	Noise sensitivity
SBM	9698 2D points	431.824	Mix direction
SPIE	4 line segments	95.101	Human-computer interaction
This paper	36 line segments	86.505	--

The number of 3D points is very large, so ICP and NDT will be too slow to use, as shown in TABLE II. 2D ICP mentioned in [13] use only 1/150 points of 3D ICP, making it very fast. Since the occlusion of the difference imaging direction or existence of defects, the contours of the workpiece have some noises. A bad registration result is obtained using 2D ICP due to these noises. In Fig.11 (a), we draw the source contours (white lines) to the reference range image with the transform matrix of 2D ICP. Because of the different contours in the black box, a bad registration occurred. As shown in Fig.11 (b), SBM will mix the direction when the template is nearly symmetric, and it the slowest method in 2D registration among these algorithms. SPIE extracts some of the typical line segments or circular arcs of the template artificially. If the template is nearly symmetrical, the direction may also be ambiguous. Our method is faster than SPIE and is robust to noises.

Due to the existing installation errors and the uneven platform, a fine registration step is necessary. This fine registration selects only dozens of points from three locations where the deformation almost never happens. In this case, locations in the target point cloud we used are the black circles in Fig.11 (d), and locations of the source point cloud can be computed by the transform matrix we get in the 2D registration step. 3D ICP is further used, and the transform matrix is refined. At last, the deformation of the workpiece can be inspected by computing the distance after aligning the source point cloud to the target point cloud. The difference image is shown in Fig.12, and the middle part is a bulge, and such a deformation is very obvious in the difference image. Besides, all the inspection steps can be finished within 100 *ms*.
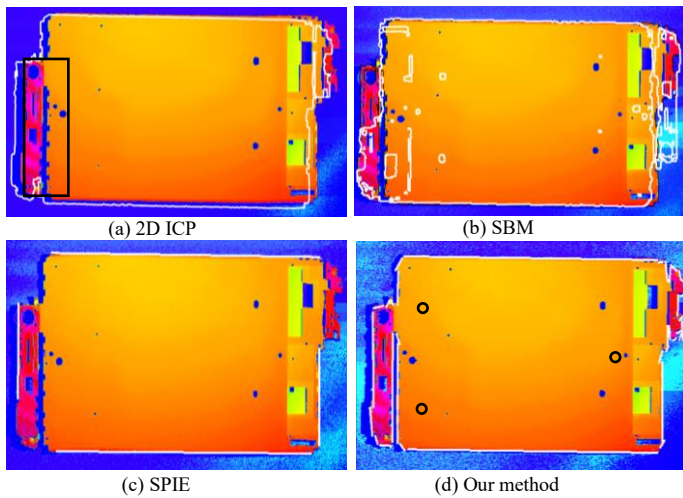

(a) 2D ICP   (b) SBM

(c) SPIE   (d) Our method
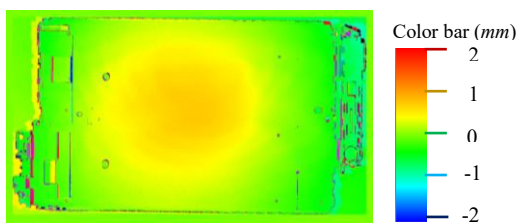
Fig.11 Registration results.

Fig.12 Inspection result.

V. CONCLUSION

A high-precision laser scanning inspection system is designed and the system precision is 0.04 *mm*. We improve the FDCM algorithm by replacing the line fitting algorithm with LSD, replacing the complex integral distance transform with a distance transform image, and using an angular Voronoi diagram. These improvements greatly simplify the two most time-consuming FDCM processes. Line segments based search also replaces the sliding window search, reducing millions of candidate locations to thousands of them. Experimental results show that 2D registration is much faster than 3D registration, and the improed FDCM is more stable than other 2D matching and registration algorithms.

REFERENCES

[1] Marshall. L. S. "Market Growing for Laser-Based Machine Vision Technologies". Photonics Spectra, 2014.

[2] Besl, P. J, and N. D. Mckay. "Method for registration of 3-D shapes." IEEE Transactions on Pattern Analysis & Machine Intelligence 14.2 .2002, pp. 239-256.

[3] Fan. Y., et al. "Study on a stitching algorithm of the iterative closest point based on dynamic hierarchy." Journal of Optical Technology 82.1 .2015: 28-32.

[4] Yuan, Chi, Xiaoqing Yu, and Ziyue Luo. "3D point cloud matching based on principal component analysis and iterative closest point algorithm." Audio, Language and Image Processing (ICALIP), International Conference on. IEEE, 2016.

[5] Magnusson, Martin. The three-dimensional normal-distributions transform: an efficient representation for registration, surface analysis, and loop detection. Diss. Örebro universitet, 2009.

[6] Mellado, Nicolas, Dror Aiger, and Niloy J. Mitra. "Super 4pcs fast global pointcloud registration via smart indexing." Computer Graphics Forum. Vol. 33. No. 5. 2014.

[7] Rusu, Radu Bogdan, Nico Blodow, and Michael Beetz. "Fast point feature histograms (FPFH) for 3D registration." Robotics and Automation. ICRA'09. IEEE International Conference on. IEEE, 2009.

[8] Liu.Ming-Yu, et al. "Fast directional chamfer matching." Computer Vision and Pattern Recognition (CVPR), IEEE Conference, 2010.

[9] http://www.vision.caltech.edu/bouguetj/calib_doc/htmls/example.html

[10] Von. Gioi, Rafael Grompone, et al. "LSD: A fast line segment detector with a false detection control." IEEE transactions on pattern analysis and machine intelligence 32.4 .2010, pp. 1 722-732.

[11] https://github.com/mingyuliutw/FastDirectionalChamferMatching

[12] Kim, Min-Koo, et al. "Automated dimensional quality assurance of full-scale precast concrete elements using laser scanning and BIM." Automation in Construction 72 .2016, pp. 102-114.

[13] Qing. H. Wu. "Study on theory and application of 3D surface defect online detection based on line-structured laser scanning". Huazhong University of Science and Technology, 2013.

[14] C. Steger, M. Ulrich, and C. Wiedemann, "Robust template matching,"in Machine Vison Algorithms and Applications. Weinheim, Germany:Wiley-VCH, 2008, pp. 222–240.

[15] Qin, Fangbo, et al. "Contour Primitives of Interest Extraction Method for Microscopic Images and Its Application on Pose Measurement." IEEE Transactions on Systems, Man, and Cybernetics: Systems 2017.